

Available online at www.sciencedirect.com

SciVerse ScienceDirect

journal homepage: www.elsevier.com/locate/he

Effects of biaxial strain on bulk 8% yttria-stabilised zirconia ion conduction through molecular dynamics

G. Dezanneau*, J. Hermet, B. Dupé

LaB. SPMS, Ecole Centrale Paris, Grande voie des vignes, 92295 Chatenay-Malabry Cedex, France

ARTICLE INFO

Article history:

Received 30 July 2011

Received in revised form

7 November 2011

Accepted 12 November 2011

Available online 24 December 2011

Keywords:

Thin films

Strain

Oxygen diffusion

Zirconia

SOFC

ABSTRACT

Tensile strain is thought to give rise to enhanced conduction properties in ion conducting compounds. However, most experimental studies in the field involve simultaneous presence of interface structures and strain, thus complicating separation of the individual effects. Here, we present molecular dynamics calculations that clarify the influence of biaxial strain in bulk yttria-stabilised zirconia. Such a study mimics what may be experimentally observed in epitaxially deposited films. We show that, as expected, tensile strain leads to enhanced ion conduction properties. The maximum enhancement is observed for a 2–3% tensile strain. We show that the increase of bulk diffusion is in part due to an opening of the Zr–Zr and Zr–Y distances induced by tensile strain, leading to a smaller oxygen migration energy. Above a 3% tensile strain, the diffusion coefficient of oxygen is strongly reduced, reaching values even lower than without strain. This decrease is associated with important structural changes of the cation and oxygen network. Also, we show that the diffusion coefficient increases by less than a factor 2 at 833 K for the optimal strain value. This confirms that the great increase of conductivity observed in zirconia/strontium titanate multilayers was due either to an electron contribution from strontium titanate or to the presence of interfaces, but not to the direct influence of strain on the oxygen diffusion coefficient in zirconia.

Copyright © 2011, Hydrogen Energy Publications, LLC. Published by Elsevier Ltd. All rights reserved.

1. Introduction

In 2008, Barriocanal et al. [1] reported that a very high ionic conductivity could be obtained in strained Yttria-Stabilised Zirconia (YSZ) films. In this case, a conductivity of 0.014 S/cm at 357 K was measured in 1 nm-thick YSZ layers, sandwiched between SrTiO₃ (STO) layers. Besides, the activation energy for conductivity was measured to be 0.64 eV. At the same temperature, bulk YSZ samples present a conductivity smaller by 8 orders of magnitude, with an activation energy of 1.1 eV. To explain such an increase of conductivity and lowering of activation energy, it was proposed that “the atomic reconstruction at the interface between highly

dissimilar structures (such as fluorite and perovskite) provides both a large number of carriers and a high-mobility”. Several authors showed that this high conductivity could also be due to an electronic contribution from the substrate or from the interlayers [2,3]. Before the publication of Ref. [1], the group of Professor Janek published several exhaustive studies concerning YSZ-containing multilayers [4,5]. These authors showed that a significant increase of ion conductivity could be obtained in a multilayer when incoherent interfaces were created between YSZ and Al₂O₃ layers [4]. In this case, the total conductivity was increased by two orders of magnitude at 848 K compared to bulk YSZ. Afterwards, they showed that multilayers with coherent interfaces [5] between Y₂O₃ and

* Corresponding author.

E-mail address: guilhem.dezanneau@ecp.fr (G. Dezanneau).

YSZ present also an increase of YSZ conductivity at 833 K. The increase represents only a factor 1.4, much smaller than the one obtained for incoherent interfaces.

All these studies, based on experiments, underlined the need for performing atomic-scale calculations to give precise information about the influence of dopant and/or local strain on the mobility of moving ions. A simulation based on *ab initio* molecular dynamics (MD) showed [6] a significant enhancement of diffusion in strained STO/YSZ multilayers, i.e. in a system similar to that of Ref. [1]. The authors estimated the ionic conductivity of the strained disordered phase to be $4 \cdot 10^6$ times higher than that of the unstrained bulk YSZ at 500 K, an increase of diffusion close to the 8 orders of magnitude reported experimentally [1]. It was also suggested that the vacancy hopping and thus the ionic conduction occurs close to the interface between YSZ and STO. The question nevertheless remained whether a significant increase of conductivity could be obtained only through strain effects, i.e. without interface. Recently, Araki and Akai [7] studied the influence of strain on YSZ conductivity through classical molecular dynamics. Their study essentially focused on the influence of uniaxial strain. They showed that the oxygen diffusion coefficient increases under tensile strain until an optimal strain value of 2%, for which an enhancement of 44% of the ion diffusion coefficient is observed at 1273 K in the direction of the imposed strain. These authors also estimated that the increase in total conductivity in a system submitted to biaxial strain could be around 60% at 1273 K. Their results, further confirmed by experiments performed on single crystals [8], gave a first indication about the expected effect of biaxial strain on bulk properties. Recently, a study based on Density Functional Theory (DFT) coupled to kinetic Monte-Carlo calculations foresaw that the conductivity would increase under biaxial tensile strain till an optimal value of 4%. The calculated oxygen diffusion coefficient for this optimal strain was greater than the one of non-strained zirconia by 3 orders of magnitude at 400 K [9]. While these two studies do not agree concerning the level of increase for oxygen diffusion coefficient upon applied strain, both report that over a certain strain value, the effect of strain is detrimental to the oxygen diffusion.

Here, we performed classical MD calculations based on semi-empirical potentials to study the influence of biaxial strain on bulk yttria-stabilised zirconia (8% of yttria). Indeed, while DFT-based approaches are gaining more and more importance, their use for a joint description of atomic-scale mechanisms and macroscopic properties such as diffusion coefficients is difficult due to CPU-time cost. Classical approaches with analytical inter-atomic potentials can fulfil such requirements as shown by Araki and Arai in the case of uniaxial strain [7]. In the present work, we studied the case of biaxial strain which mimics exactly what is observed in fully coherent epitaxial layers. We did not include any interfaces with other materials in order to limit our study to pure strain effects.

2. Calculation details

All simulations were run with the DLPOLY code [10,11] using a supercell of $6 \times 6 \times 6$ unit cells (containing 734 Zr, 130 Y, 1663

oxygen atoms and 65 oxygen vacancies). This corresponds to the chemical formula $Zr_{0.85}Y_{0.15}O_{1.925}$ close to the so-called 8YSZ. Interactions between ions were described by a long-range Coulombic term calculated by Ewald Summation, and a short-range Buckingham pair potential. For Coulombic interactions, the formal charges +4, +3 and –2 were used respectively for Zr, Y and O ions. The use of formal ionic charge was shown to represent correctly the dynamic features of atoms in most oxide compounds. The Buckingham potential is described by:

$$\varphi_{ij}(r) = A_{ij} \exp\left(-\frac{r}{\rho_{ij}}\right) - \frac{C_{ij}}{r^6} \quad (1)$$

where r is the distance between the atoms i and j , and A_{ij} , ρ_{ij} , C_{ij} are potential parameters specific to each ion pair whose values are given in Table 1. The set of potentials was taken from previous studies, which were shown to reproduce most of the features of yttria-stabilised zirconia [12–14].

For non-strained supercells, the system was first equilibrated at 1300, 1600 and 1900 K and at zero pressure for 20,000 time steps (with a time step of 0.5 fs) in the isothermal–isobaric (NPT) ensemble with Nosé–Hoover thermostat. Then 100,000 time steps allowed finding the equilibrium lattice parameters. These lattice parameters are $a = 31.20766 \text{ \AA}$, $a = 31.27444 \text{ \AA}$, $a = 31.34508 \text{ \AA}$ respectively at 1300, 1600 and 1900 K. These cell parameters were then used to define the strain at each temperature. The strained structures were created by imposing the strain simultaneously in the a and b directions. A positive strain means that a and b are put in tension, i.e. under a tensile strain. The strain value represents thus the relative increase, expressed in percentage, of the a and b cell parameters if compared to the zero-strain situation. Similarly, a negative strain value corresponds to a compression for the a and b cell parameters, and expresses the relative difference (decrease), expressed in percentage, of the a and b cell parameters, taking the zero-strain situation as the reference. After a and b were set corresponding to a given strain value, simulations were performed in the NVT mode and the c parameter was adjusted until obtaining a zero pressure along the c direction. Long simulations, typically corresponding to 100,000 till 200,000 steps in the NVT mode, were necessary for high strain values due to significant cationic displacements. Then, NVE simulations were realised during 1,000,000 to 2,000,000 time steps.

3. Results

After NVT calculations, we can represent the deformation of the system with biaxial strain, i.e. the evolution of the c

Table 1 – Inter-atomic Buckingham potentials used for molecular dynamics calculations for Zr–O, Y–O, O–O pairs of atoms [12–14].

Interaction	A (eV)	ρ (Å)	C (eV Å ⁶)
Y ³⁺ –O ^{2–}	1766.40	0.33849	19.43
Zr ⁴⁺ –O ^{2–}	1502.11	0.3477	5.1
O ^{2–} –O ^{2–}	9547.96	0.2192	32.0

parameter as a function of strain. This evolution is shown in Fig. 1 and presents, for intermediate strain values, a linear evolution of the c parameter with strain. It is known that if a biaxial strain is applied along a and b directions in a material, an elastic deformation occurs along the c direction according to the following equation:

$$\frac{\Delta c}{c_0} = \left(\frac{-2\nu}{1-\nu} \right) \cdot \frac{\Delta a}{a_0} \quad (2)$$

where $\Delta a/a_0$ and $\Delta c/c_0$ are the deformations along the a (equal to b) and the c direction respectively and ν is the Poisson coefficient. For strain values between -4% and $+3\%$, the evolution of the c parameter follows very well the law described by equation (2) with a Poisson coefficient equal to 0.18 (see Fig. 1), a bit smaller than measured experimentally around 0.25 [14]. For strain values below -4% and exceeding $+3\%$, the deformation along the c direction deviates from what is expected from equation (2). This indicates that, for these high (absolute) strain values, the material changes substantially and the elastic approximation for the material response to biaxial strain is no longer valid.

From NVE simulations, we observed that oxygen atoms diffuse during the simulation as reflected by their mean square displacement versus time (Fig. 2a). From this curve, it is possible to extract the oxygen diffusion coefficients, after fitting the mean square displacements of oxygen atoms as a function of time, applying the Einstein law.

$$\langle |r_i(t) - r_i(0)|^2 \rangle = 6Dt + \text{constant} \quad (3)$$

where $|r_i(t) - r_i(0)|$ is the displacement of the oxygen atom i from its initial position, t is the simulation time, D is the oxygen diffusion coefficient. The constant value is generally associated with the purely vibrational motion of atoms around the crystallographic sites. In our case, the diffusion

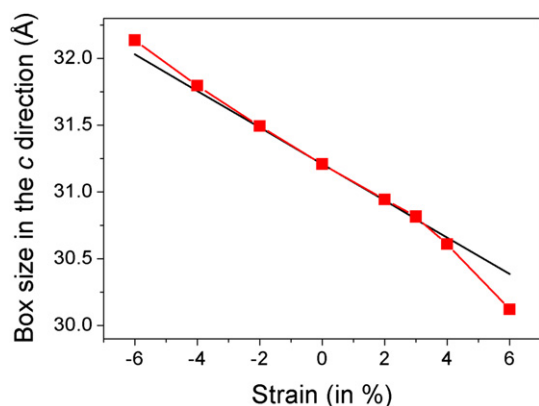


Fig. 1 – Evolution of the simulation box size in the c direction as a function of the biaxial strain applied along a and b directions at $T = 1300$ K. The black line corresponds to what expected from elastic calculations with a $\nu = 0.18$ Poisson coefficient. The red squares correspond to the results of simulations. (For interpretation of the references to colour in this figure legend, the reader is referred to the web version of this article.)

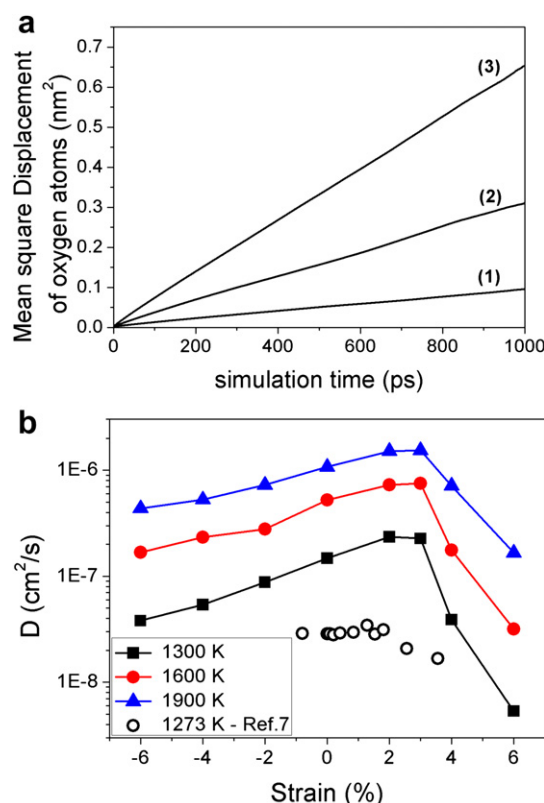


Fig. 2 – (a) Mean square displacement of oxygen atoms at (1) 1300 K (2) 1600 K and (3) 1900 K. (b) Oxygen diffusion coefficients deduced from MD calculations, as a function of biaxial strain at 1300 K (black square and line), 1600 K (red circles and line), 1900 K (blue triangles and line). Oxygen diffusion coefficients at 1273 K as a function of uniaxial strain from Ref. [7] (circles). (For interpretation of the references to colour in this figure legend, the reader is referred to the web version of this article.)

coefficient was fitted in the 500–1000 ps time range, for which a linear behaviour was observed. Such diffusion coefficients are plotted in Fig. 2b. We also present on this graph the oxygen diffusion coefficients as obtained by Araki and Arai [7] as a function of uniaxial tensile strain. Their results differ from ours at zero strain because of different potentials used for simulating the doped zirconia. Our results indicate that the diffusion coefficient passes through a maximum around $+2$ – 3% of tensile biaxial strain. Below this maximum, the diffusion coefficient evolves continuously with applied strain, i.e. diminishes for compressive strain and increases for tensile strain when compared to the zero-strain value. Above this 3% of tensile strain, the diffusion coefficient drops suddenly reaching values even lower than those found for compressive strain. A similar evolution was observed when applying uniaxial strain as shown in Fig. 2b from Araki's results [7]. In both cases, the greatest increase of diffusion coefficient was observed in the direction of applied strain, i.e. along c direction for uniaxial strain and in the (a,b) plane in the present study. We calculated the diffusion coefficient under tensile strain to be between 1.5 and 2 greater along a and b directions

than along c direction. Under compressive strain, the difference was smaller, the diffusion coefficient along c direction exceeding that of a and b directions by only 10%. This means that the biaxial strain logically induces anisotropy in the diffusion process.

The evolution of D coefficient with strain is observed for the three temperatures considered here, i.e. for 1300, 1600 and 1900 K. D can be expressed as a function of temperature T through:

$$D(T) = D_0 \cdot \exp(-E_A/k_B T) \quad (4)$$

k_B being the Boltzmann constant, D_0 a pre-exponential factor and E_A the activation energy of the diffusion process. These activation energies are plotted in Fig. 3. For strain values lower than +3% of tensile strain, the activation energy for oxygen migration increases slightly with compressive strain and diminishes with tensile strain. The lowest activation energies values are obtained for the +2% and +3% strain values. For higher strain values, the activation energy for oxygen diffusion increases suddenly indicating a change in the conduction mechanism.

In order to explain the evolution of conductivity with applied strain, we extracted some information on the local environment of atoms. In the fluorite structure, the shorter metal–metal pairs lie in the [1, 1, 0], [1, 0, 1] and [0, 1, 1] directions. These metal–metal pairs are important for the oxygen diffusion since oxygen atoms jump from one site to another, skipping between these cations (see Ref. [13] for a general discussion on these aspects). When the strain value increases from –6% till 6%, all the Zr–Zr and Zr–Y distances increase continuously with strain, whatever the crystallographic direction considered (Fig. 4). Indeed, even for pairs having a z component, the increase in the a and b directions is more important than the slight decrease along the c direction, leading to an overall metal–metal distance increase. This increase of metal–metal distance may in part explain the favoured diffusion and lower activation energy for oxygen transport under tensile strain.

However, since this metal–metal distance continues to increase for tensile strain higher than 3%, this parameter is not sufficient to explain the evolution of diffusion properties for high strain values. If we focus on the metal–oxygen

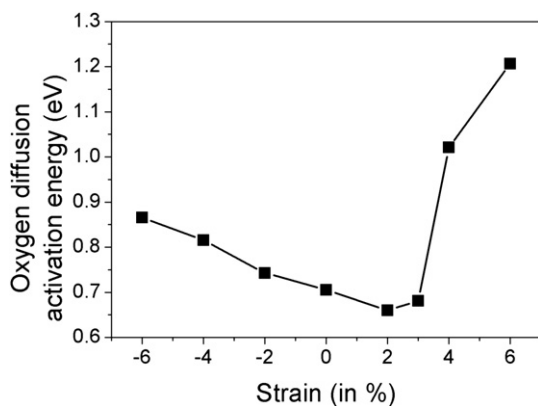


Fig. 3 – Activation energy for oxygen diffusion as a function of biaxial strain.

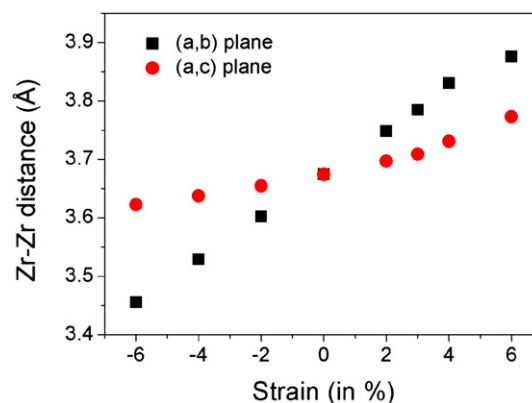


Fig. 4 – Evolution of Zr–Zr distance as a function of strain for pairs of atoms located in a (a, b)- like or (a, c)-like plane.

distance, it increases continuously between –6% and +3% applied strain, while it starts diminishing for higher strain values (see Fig. 5b and a). Parallely to this, the environment of cations evolves strongly with strain as shown in Fig. 6a and b. These figures represent the coordination number of Zr and Y cations, taken as the number of oxygen neighbours inside a sphere of radius r . For –6% to +3% strain values, the Zr and Y coordination numbers follow what expected in a disordered

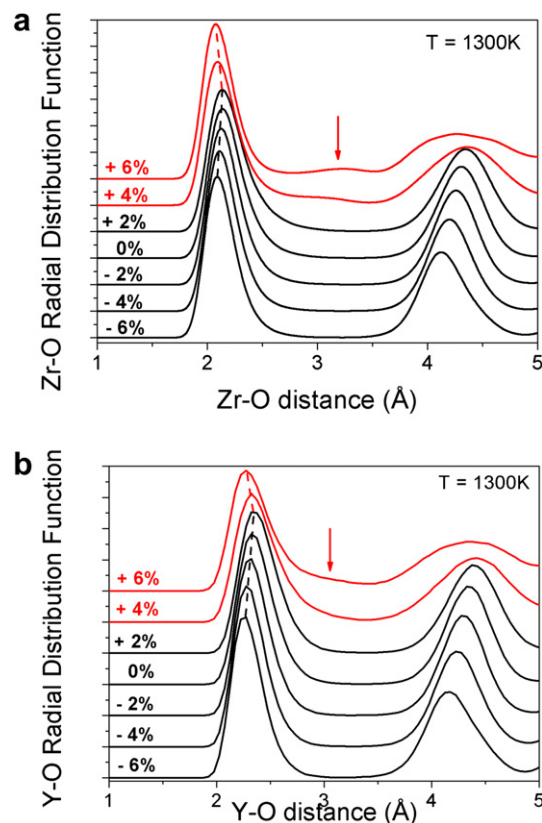


Fig. 5 – Evolution of (a) Zr–O and (b) Y–O Radial Distribution function for different values of biaxial strain. Dashed lines have been added to follow the first shell peak maximum. The arrow corresponds to the hypothetical second shell (see text).

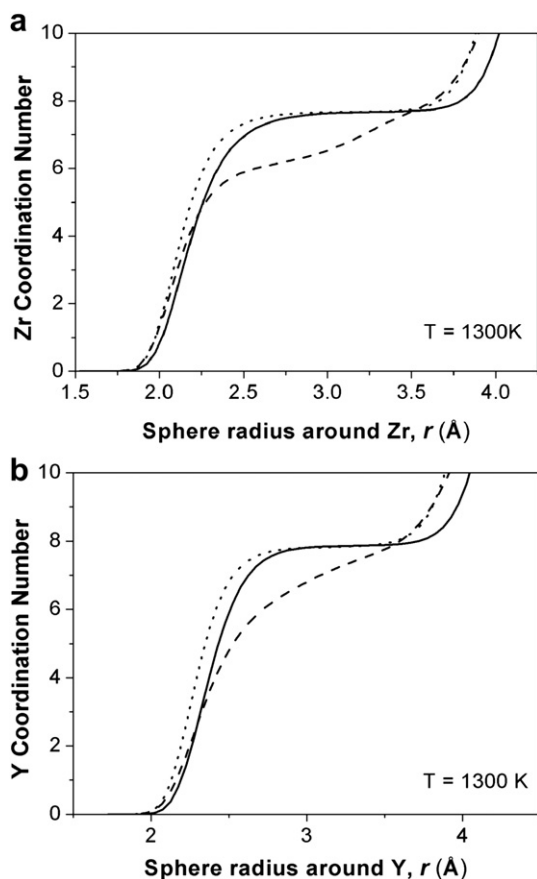


Fig. 6 – Coordination number of (a) Zr and (b) Y atoms as a function of the integration sphere radius r around Zr/Y atoms for different values of strain: -6% (dot line), 0% (solid line), +6% (dash line).

fluorite-like compound, i.e. are close to 7.7 for the first shell. For higher strain values, the environment of cations is much more distorted. In the case of Zr atoms, it seems that their coordination number reaches a value of 6, these six oxygen atoms constituting the first shell and then other oxygen atoms locate at a distance of 3 Å that would constitute a second shell. This second shell, indicated by an arrow in Fig. 5a and b, is more pronounced in the case of zirconium than in the case of yttrium, in part due to the naturally longer distance of yttrium–oxygen distance for the first shell. From these two facts, it is clear that the local structure around cations from -6% till +3% strain is that of the fluorite structure while for higher strain values, the local environment of cations is not the one expected for a pure fluorite structure. In this case, the observed shorter metal–oxygen distance is coherent with the smaller coordination number found and with the possible existence of two coordination shells.

As reported in Ref. [7], for high strain values, the structure is strongly distorted and does not longer appear to be fluorite-like. The main signature of this distortion is the misalignment of cation atoms, observed here and also reported in Refs. [6,7], in opposite to their perfect alignment in the fluorite structure. Since the topology of sites and local order are no longer those of a fluorite structure, the equivalency of oxygen sites is no

longer true which might induce a decrease of oxygen diffusion coefficient. Here, the consideration of oxygen diffusion through oxygen vacancies, valid in fluorite-like compounds, is probably no longer true for highly strained structures.

4. Discussion

A general framework for the understanding of the strain effect on diffusion properties in thin films was given few years ago in several articles from Professor Janek's group [4,5,16,17]. It was first shown that a dilative strain could be seen as a negative pressure and would lead in all cases to enhanced conduction properties, since oxygen would have more volume for migration. In this case, a linear dependency was calculated for the logarithm of conductivity of the strained material versus the level of strain. Such a dependency was also found here as shown in Fig. 2b. If we extrapolate our results to a temperature of 833 K (an extrapolation method was used because of poor statistics at low temperature), we find an evolution of the diffusion coefficient as a function of strain very similar to the one obtained experimentally for conductivity (cf. Fig. 7). The increase of diffusion/conductivity in these two cases is small, being less than a factor 2.

On the other side, if the increase of diffusion coefficient found in the present work is similar to the one observed by Akari and Akai considering uniaxial strain, it differs strongly from the value calculated in Ref. [9]. This study consisted in Kinetic Monte–Carlo calculations based on a set of migration energies determined by DFT. From a general point of view, both approaches should give similar results. One could argue that many approximations are made during the building of KMC scheme. Nevertheless, only jumps with low probability are neglected and this should not affect the final result. The size of the system may also affect the reliability of results in DFT-based calculations. Another argument could be that the topology of the material changes for high strain values and

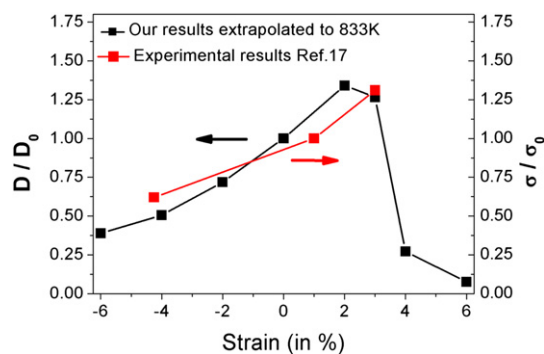


Fig. 7 – Relative oxygen diffusion coefficients as extrapolated to 833 K from simulations (black line and symbols), and relative conductivity measured from experiments in 8YSZ/M₂O₃ multilayers from Ref. [15] (red line and symbols). D_0 and σ_0 refer to simulated diffusion coefficient and experimental conductivity of 8YSZ without strain. (For interpretation of the references to colour in this figure legend, the reader is referred to the web version of this article.)

then possible pathways are badly reproduced. Nevertheless, this is the case for high strain values not for the optimal strain that was shown to keep the fluorite structure. On the other hand, one may argue that semi-empirical potentials due to their simplicity cannot reproduce with precision the behaviour of zirconia under high strain values. This explanation could be in part supported by the difference between calculated ($\nu = 0.18$) and experimental ($\nu = 0.25–0.30$ [15]) Poisson coefficient. Nevertheless, the present results based on semi-empirical potentials show a good agreement with experiment as shown in Fig. 7. As a conclusion, it is difficult to determine which of the two studies gives the best accuracy for evaluating the diffusion increase with strain. On the other side, both studies indicate that, beyond a given biaxial strain value (3% in our case, 4% in Ref. [9]), the applied strain worsens the diffusivity. Indeed, the DFT calculations of Ref. [9] showed that for these high strain values, the cation–oxygen bond was strengthened leading to an increase of migration energy, as observed in this work.

We then suggest that further calculations could be performed to give a definite and quantitative answer on the effect of strain in zirconia. A first study could consist in reproducing the KMC study of Ref. [9], using migration energies as calculated from semi-empirical potentials. This would allow determining whether the difference come from the methodology employed or from the different ways (semi-empirical or DFT approach) to calculate the migration energies. Another possible study could consist in performing DFT molecular dynamics simulations on strained cells, with a level of statistics that allow for diffusion coefficient determination.

5. Conclusion

From these results concerning MD calculations of strained YSZ, we can thus affirm that the presence of a biaxial tensile strain could effectively lead to an increased conductivity in zirconia. Also, we have shown that the maximum of conductivity is obtained for an optimal tensile strain value that is found to be around 2–3% for 8% yttria-doped zirconia. This value is slightly smaller than the one foreseen previously from DFT calculations, around 4% [6]. The level of increase is expected to be less than a factor 2, much smaller than found in a previous article but in good agreement with some experimental results. Beyond this optimal strain value, the structure becomes highly distorted if compared to the original fluorite structure and the nature of the oxygen–cation bonding evolves leading to strengthened cation–oxygen bond, which then decreases the oxygen diffusion coefficient. Then, this supports the conclusions from Refs. [4,5], that a significant enhancement of conductivity could only be obtained when semi-coherent interfaces are obtained within multilayers, i.e. when dislocations appear at the interface.

REFERENCES

- [1] Garcia-Barricocal JG, Rivera-Calzada A, Varela M, Sefrioui Z, Iborra E, Leon C, et al. Colossal ionic conductivity at interfaces of epitaxial $\text{ZrO}_2\text{:Y}_2\text{O}_3/\text{SrTiO}_3$ heterostructures. *Science* 2008;321:676.
- [2] Guo X. Comment on “colossal ionic conductivity at interfaces of epitaxial $\text{ZrO}_2\text{:Y}_2\text{O}_3/\text{SrTiO}_3$ heterostructures. *Science* 2009; 324:465.
- [3] Cavallaro A, Burriel M, Roqueta J, Jaume Apostolidis A, Bernardi A, Tarancon A, et al. Electronic nature of the enhanced conductivity in YSZ-STO multilayers deposited by PLD. *Solid State Ionics* 2010;181:592–601.
- [4] Peters A, Korte C, Hesse D, Zakharov N, Janek J. Ionic conductivity and activation energy for oxygen ion transport in superlattices – the multilayer system CSZ (ZrO_2+CaO)/ Al_2O_3 . *Solid State Ionics* 2007;178:67–76.
- [5] Korte C, Peters A, Janek J, Hesse D, Zakharov N. Ionic conductivity and activation energy for oxygen ion transport in superlattices – the semicoherent multilayer system YSZ ($\text{ZrO}_2+9.5 \text{ mol\% Y}_2\text{O}_3$)/ Y_2O_3 . *Phys Chem Chem Phys* 2008;10: 4623–35.
- [6] Pennycook TJ, Beck MJ, Varga K, Varela M, Pennycook SJ, Pantelides ST. Origin of colossal ionic conductivity in oxide multilayers: interface induced sublattice disorder. *Phys Rev Lett* 2010;104. art. N°115901.
- [7] Araki W, Arai Y. Optimum strain state for oxygen diffusion in yttria-stabilised zirconia. *Solid State Ionics* 2011;190:75–81.
- [8] Araki W, Kuribara M, Arai Y. Effect of uniaxial stress on ionic conductivity of 14 mol%-yttria-stabilized zirconia single crystal. *Solid State Ionics* 2011;193:5–10.
- [9] Kushima A, Yildiz B. Oxygen ion diffusivity in strained yttria stabilized zirconia: where is the fastest strain? *J Mater Chem* 2010;20:4809–19.
- [10] DL_POLY classic code: http://www.ccp5.ac.uk/DL_POLY_CLASSIC/.
- [11] Smith W, Forester TR, Todorov IT. The DL_POLY classic user manual, Daresbury Laboratory, United Kingdom.
- [12] Minervini L, Zacate M, Grimes RW. Defect cluster formation in M_2O_3 -doped CeO_2 . *Solid State Ionics* 1999;116:339–49.
- [13] Zacate MO, Minervini L, Bradfield DJ, Grimes RW, Sickafus KE. Defect cluster formation in M_2O_3 -doped cubic ZrO_2 . *Solid State Ionics* 2000;128:243–54.
- [14] Tarancón A, Morata A, Peiró F, Dezanneau G. A molecular dynamics study on the oxygen diffusion in doped fluorites: the effect of the dopant distribution. *Fuel Cells* 2011;11: 26–37.
- [15] Fujikane M, Setoyama D, Nagao S, Nowak R, Yamanaka S. Nanoindentation examination of yttria-stabilized zirconia (YSZ) crystal. *J Alloys Compounds* 2007;431:250–5.
- [16] Korte C, Schichtel N, Hesse D, Janek J. Influence of interface structure on mass transport in phase boundaries between different ionic materials experimental studies and formal considerations. *Monatsh Chem* 2009;140:1069–80.
- [17] Schichtel N, Korte C, Hesse D, Janek J. Elastic strain at interfaces and its influence on ionic conductivity in nanoscaled solid electrolyte thin films-theoretical considerations and experimental studies. *Phys Chem Chem Phys* 2009;11:3043–8.